

Protein Diversity Confers Specificity in Plasmid Segregation

Timothy J. G. Fothergill, Daniela Barillà, and Finbarr Hayes*

Faculty of Life Sciences, University of Manchester, Manchester, England

Received 4 October 2004/Accepted 10 January 2005

The ParG segregation protein (8.6 kDa) of multidrug resistance plasmid TP228 is a homodimeric DNA-binding factor. The ParG dimer consists of intertwined C-terminal domains that adopt a ribbon-helix-helix architecture and a pair of flexible, unstructured N-terminal tails. A variety of plasmids possess partition loci with similar organizations to that of TP228, but instead of ParG homologs, these plasmids specify a diversity of unrelated, but similarly sized, partition proteins. These include the proteobacterial pTAR, pVT745, and pB171 plasmids. The ParG analogs of these plasmids were characterized in parallel with the ParG homolog encoded by the pseudomonas plasmid pVS1. Like ParG, the four proteins are dimeric. No heterodimerization was detectable in vivo among the proteins nor with the prototypical ParG protein, suggesting that monomer-monomer interactions are specific among the five proteins. Nevertheless, as with ParG, the ParG analogs all possess significant amounts of unordered amino acid residues, potentially highlighting a common structural link among the proteins. Furthermore, the ParG analogs bind specifically to the DNA regions located upstream of their homologous *parF*-like genes. These nucleoprotein interactions are largely restricted to cognate protein-DNA pairs. The results reveal that the partition complexes of these and related plasmids have recruited disparate DNA-binding factors that provide a layer of specificity to the macromolecular interactions that mediate plasmid segregation.

Protein machines for DNA transactions, including transcription, replication, recombination, and segregation, involve highly specific protein-protein and protein-nucleic acid contacts. These interactions are crucial for the precise assembly of the requisite multiprotein complexes and for the biological processes that these complexes mediate (1). A broad, but defined, spectrum of protein-protein and protein-DNA interactions have evolved that determine exactly the architecture of nucleoprotein complexes (5, 30, 43 [and other references therein]).

The segregation of plasmids in bacteria also involves specific protein-protein and protein-DNA interactions. Plasmid partition most commonly involves a pair of plasmid-encoded proteins, often denoted ParA and ParB, that assemble on a *cis*-acting partition site, sometimes known as *parS* (39). The ParA protein does not directly contact the partition site DNA but is instead recruited into the partition nucleoprotein complex through interactions with the ParB protein (4, 6). ParA possesses weak intrinsic ATPase activity which is stimulated by the ParB factor. The assembly of the partition nucleoprotein complex is required for the proper movement of plasmid pairs in opposite poleward directions prior to cell division (9, 15, 26, 27). This movement is likely to occur as a result of extensive ATP-mediated polymerization and/or depolymerization of the ParA component (D. Barillà et al., EMBO J., in press).

The partition cassette of the multidrug resistance plasmid TP228 specifies a ParA homolog, ParF, that is approximately half the size of the prototypical ParA protein encoded by plasmid P1. In addition, the TP228 system includes the ParG protein (8.6 kDa) instead of ParB (18). ParG is dimeric and

interacts with sequences upstream of *parFG*; this interaction is modulated either positively or negatively by ParF in a ratio-dependent manner (4). The ParG dimer consists of a folded domain made up of two tightly intertwined C-terminal domains, one from each protomer, combined to form a single hydrophobic core, and two flexible tails consisting of N-terminal regions of both subunits. The folded parts of the subunits are related by a local twofold rotation axis, and they each consist of one β -strand and two α -helices. The two β -strands form an intermonomer twisted antiparallel β -structure, with four α -helices packed together on one side of this β -structure. Thus, the folded part of ParG has a ribbon-helix-helix architecture similar to that of the Arc/MetJ superfamily of DNA-binding transcriptional repressors, although the primary sequence similarity with Arc/MetJ is very low (14).

The archetypal ParA and ParB proteins of the P1 plasmid are 44.3 and 37.4 kDa, respectively. Many plasmids encode similarly sized, homologous partition proteins, but one widely disseminated subgroup of the ParA superfamily, which is typified by ParF, consists of homologs that are approximately half the size of P1 ParA. Intriguingly, the genes for these half-sized homologs are accompanied downstream not by *parB*-type genes but instead by a diversity of open reading frames that encode proteins with masses of ~8 to 11 kDa (18). Some of these open reading frames, such as that located on plasmid pVS1 (21), are predicted to specify homologs of ParG, whereas others encode proteins that apparently are entirely unrelated either to ParG or to each other (18). For example, the partition regions of plasmids pTAR and pB171 include homologs of *parF*, but the downstream genes are homologous neither to *parB*, to *parG*, nor to each other (Fig. 1A) (18, 23, 40). Similarly, the putative partition cassette of plasmid pVT745 contains a *parF*-like gene whose 3' end overlaps the 5' end of yet another novel downstream gene (11). Here the interaction specificities of the products of these diverse downstream genes

* Corresponding author. Mailing address: Faculty of Life Sciences, University of Manchester, Jackson's Mill, P.O. Box 88, Sackville St., Manchester M60 1QD, England. Phone: 44 161 3068934. Fax: 44 161 2360409. E-mail: finbarr.hayes@manchester.ac.uk.

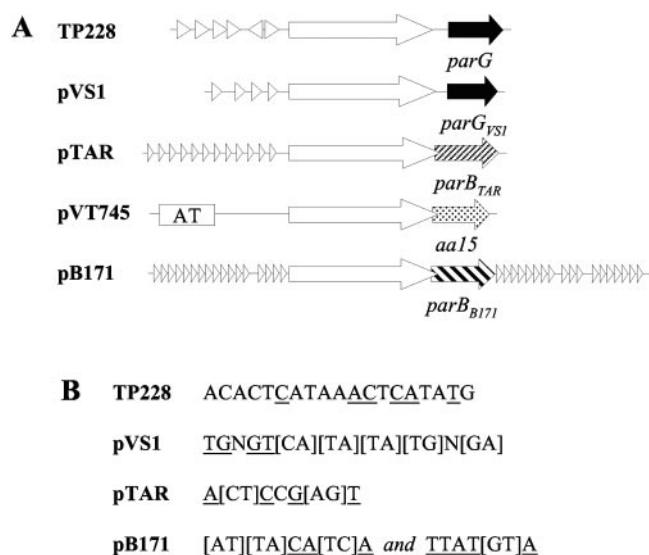


FIG. 1. Organization of the TP228, pVS1, pTAR, pVT745, and pB171 partition systems. (A) Genetic structures of the partition cassettes. Each cassette includes a *parF* homolog (open arrow) and a flanking gene downstream (18). The *parG* and *parG_{VSI}* genes are homologs (14, 18). In contrast, the *parB_{TAR}*, *aa15*, and *parB_{B171}* genes are unrelated to *parG* or to each other (18). Each cassette is flanked by repeat sequences (arrowheads) that differ in number, location, and sequence between each plasmid (4, 8, 12). (B) The consensus sequences in TP228 (4), pVS1, pTAR (12), and pB171 (8) are shown. The pVT745 region contains an AT-rich (~80%) region that includes a number of repeat sequences.

are analyzed. The proteins bind to their cognate putative partition sites, but this interaction and the self-association of the proteins is largely specific. Thus, although these systems share common ParF-type proteins, disparate partner proteins have been recruited as specificity determinants. This evolutionary strategy ensures that cross talk is minimized between partition systems from different plasmids.

MATERIALS AND METHODS

Bacterial strains and plasmids. *Escherichia coli* was grown in Luria-Bertani medium with ampicillin (50 µg/ml) or chloramphenicol (10 µg/ml) selection when appropriate. *E. coli* DH5α (42) was used for plasmid propagation and cloning. Strain BL21(DE3) (Invitrogen) was used for protein production. *E. coli* SP850 (*Δcyo*) (37) was used in two-hybrid analysis (4). Strain BR825 is *polA* (29) and was used in plasmid partition assays.

Plasmids pUCD550 (13), pME6010 (21), pKN2 (31), and pB171-S (40), which were used as sources of the pTAR, pVS1, pVT745, and pB171 partition regions, were kindly provided by M. Yarmolinsky, S. Heeb, D. Galli, and T. Tobe, respectively. Oligonucleotide primers used for PCR amplification of these regions or subfragments are listed in Table 1. The partition regions were amplified by PCR and cloned in the partition assay vector, pFH450 (17), to test for segregational stability, except for the partition region of pTAR, which was subcloned as a BamHI fragment from pUCD550 in the same site in pFH450. For incompatibility assays, appropriate restriction fragments harboring the partition regions were subcloned in pUC18 plasmids from pFH450 derivatives. In addition, the pMB1 replicon was deleted from pFH450-based plasmids by digestion with AseI and SalI, filling of the overhangs with Klenow fragment, and religation of the larger fragment that includes the P1 replicon, chloramphenicol resistance gene, and the partition region, thereby producing plasmids that replicated exclusively by the low-copy-number P1 replicon and were stabilized by the partition region of interest. For two-hybrid assays (24), *parG* homologs and analogs were PCR amplified and inserted in both the pT18 and pT25 two-hybrid vectors in frame with the T18 and T25 fragments of *Bordetella pertussis* adenylate cyclase. In each case, the PCR fragments were cloned between the KpnI and HindIII

sites of pT18 and between the BamHI and KpnI sites of pT25. The *parG* analogs were also cloned between the NdeI and NotI or XhoI sites in the pET-22b(+) overexpression vector (Novagen) for the production of His-tagged proteins.

Bacterial two-hybrid analysis. The bacterial two-hybrid scheme based on reconstitution of adenylate cyclase activity in *E. coli* was used to monitor interactions among partition proteins (24). One bait and one prey plasmid were co-transformed pairwise into *E. coli* SP850, and the cells were plated on Luria-Bertani plates containing ampicillin and chloramphenicol and incubated at 30°C for 36 to 48 h. Single colonies were then streaked onto MacConkey-maltose agar plates, grown at 30°C, and monitored over a 48-h period for development of a red color indicative of a protein-protein interaction.

Plasmid partition and incompatibility assays. The partition regions of interest were cloned in the pFH450 vector that harbors the P1 unit copy number and pMB1 moderate copy number replicons and a chloramphenicol-resistance-selective marker (17). In a wild-type host, pFH450 replicates by the pMB1 origin and can be isolated and manipulated with ease. However, in a *polA* host, the pMB1 origin is nonfunctional and replication switches to a low copy number under the control of the P1 replicon. As the plasmid does not possess accessory stability genes, it is unstable in this host in the absence of selective pressure. The efficacy of the inserted regions in promoting partition of pFH450 in the BR825 *polA* strain was measured after growth under nonselective conditions for ~25 generations, as detailed elsewhere (18). Incompatibility assays were performed by using partition regions cloned in pUC18 (44) and with derivatives of pFH450 that replicated exclusively by the low-copy-number P1 replicon and contained the partition regions of interest. Incompatibility tests were performed as outlined previously (18).

Protein production and purification. His-tagged proteins were overproduced in *E. coli* BL21(DE3) and purified by Ni²⁺ affinity chromatography according to the Novagen technical manual. His-tagged ParG was similarly purified (4).

Chemical cross-linking. Cross-linking reactions with dimethyl pimelimidate (DMP) (10 mM) were performed at protein concentrations of 0.15 to 0.5 mg/ml in reaction buffer (50 mM HEPES-KOH [pH 8.5], 50 mM KCl, 5 mM MgCl₂) as outlined previously (4).

DNA binding assays. DNA binding assays were performed essentially as described previously (4). In brief, 5'-end-biotin-labeled DNA fragments, corresponding to the regions ~250 to 300 bp upstream of the *parF* translation start sites, were obtained by PCR amplification with 5'-end-biotin-labeled oligonucleotides. Binding reaction mixtures (20 µl) included the end-labeled DNA fragment (1 to 2 nM), recombinant ParG analogs (quantities as specified in figure legends), and 1 µg of poly(dI-dC) in binding buffer (10 mM Tris-HCl [pH 7.5], 50 mM KCl, 1 mM dithiothreitol, 2.5% glycerol, 5 mM MgCl₂). Reaction mixtures were incubated for 20 min at room temperature and separated on a 1% agarose gel in 0.5× Tris-borate-EDTA at 100 V. The gel was blotted onto a positively charged nylon membrane (Roche) for 1 h, and the transferred DNA fragments were immobilized onto the membrane by UV cross-linking. Detection of the biotinylated DNA was performed with the LightShift chemiluminescent electrophoretic mobility shift assay kit (Pierce).

Sedimentation velocity analysis. Sedimentation velocity analysis was performed as described previously (4) in an Optima XL-I ultracentrifuge (Beckman) at a speed of 60,000 rpm and a temperature of 23°C. Radial scans were acquired at 280 nm. The results were analyzed by g(s*) analysis with the program DCDT+, version 1.13 (32).

Circular dichroism spectroscopy. Protein solutions were diluted to ~10 nM in 10 mM NaCl–5 mM sodium phosphate (pH 7.0), and ellipticity was measured in a quartz cell with a 0.5-cm path length. Circular dichroism measurements were performed with a Jasco J-810 spectropolarimeter from 190 to 260 nm at 25°C. Each scan is the average of at least four accumulations and is corrected against buffer-only spectra. Data were analyzed on the DichroWeb website (28, 41) with CONTIN and CDSSTR software (7, 33, 38).

RESULTS

Partition cassettes of plasmids TP228, pVS1, pTAR, pVT745, and pB171. Plasmids TP228, pVS1, pTAR, pVT745, and pB171 originate from *Salmonella enterica* serovar Newport, *Pseudomonas aeruginosa*, *Agrobacterium tumefaciens*, *Actinobacillus actinomycetemcomitans*, and *E. coli*, respectively. The partition cassettes of these plasmids specify homologs of the archetypal ParA protein encoded by the P1 plasmid, but these homologs are approximately one-half the size of the P1

TABLE 1. Oligonucleotide primers used

Primer ^a	Sequence (5'-3') ^b
pVS1-450f	ACTACTACTGATATCTCGAGCGTTCCTAATCATC (559)
pVS1-450r	GTGTGTGTGGTTCGACGCCTCAACTTCTCCACCAG (1635)
pVS1-ETf	GGTGGTGGCATATGAGCAAAAGCACAAAC (1830)
pVS1-ETr	GGGAAACTCGAGCTCTGGTAGCTGCGC (2042)
pVS1-T18f	ATATATGGTACCTATGAGCAAAAGCACAAAC (1830)
pVS1-T18r	TAATTAAGCTTATCTCTGGTAGCTGCGC (2042)
pVS1-T25f	ATTAAGGATCCCATGAGCAAAAGCACAAAC (1830)
pVS1-T25r	ATATTGGTACCCCTTACTCTGGTAGCTG (2045)
pTAR-ETf	TTATTATACATATGAATGATTTCAAAC (936)
pTAR-ETr	TATATTGCGGCGCTCCTTTGGCCTCCAA (1217)
pTAR-T18f	ATATTAGGATCCCATGAATGATTTCAAAC (936)
pTAR-T18r	ATATAAAGCTTATTCCTTTGGCCTCCAA (1217)
pTAR-T25f	ATATTAGGATCCCATGAATGATTTCAAAC (936)
pTAR-T25r	ATATATGGTACCCCTCATCCTTTGGCCTC (1220)
pVT745-450f	AATATTAATATGCATCGGTGAAAGCGAAAAGAAAC (12975)
pVT745-450r	AATAATAAAGTTAACC GCCAGACAACAACAAAATG (10677)
pVT745-ETf	TATATATACATATGAGTAAATTAACAAAA (11647)
pVT745-ETr	TATATACTCGAGTAACATGCCTTTTTC (11411)
pVT745-T18f	ATAAATGGTACCTATGAGTAAATTAACAAAA (11647)
pVT745-T18r	TTTTTAAGCTTATTAACATGCCTTTTTC (11411)
pVT745-T25f	ATAAAGGATCCCATGAGTAAATTAACAAAA (11647)
pVT745-T25r	ATATTGGTACCCCTCATAACATGCCTTT (11408)
pB171-450f	GACTCACTCGAGTGGTGTGCTAACTTCATCATACG (58278)
pB171-450r	TGTGTGGATATCTCAGCTCAACGGAGGTCTAC (59863)
pB171-ETf	CTCTCTCATATGGTGAAGAAACCCAGC (59332)
pB171-ETr	AGAGAGCTCGAGCGTTAGTGTTTTTAA (59604)
pB171-T18f	ATATATGGTACCTATGGTGAAGAAACCCAGC (59332)
pB171-T18r	ATATAAAGCTTATCGTTAGTGTTTTTAA (59604)
pB171-T25f	ATAAAGGATCCCATGGTGAAGAAACCCAGC (59332)
pB171-T25r	ATATATGGTACCCCTTACGTTAGTGTTTT (59607)

^a Oligonucleotides with suffixes 450, ET, T18, and T25 indicate primers that were used for amplifying products for cloning in pFH450, pET22(b)+, pT18, and pT25, respectively. The letters f and r indicated forward and reverse primers.

^b Primer sequences were based on GenBank accession numbers AF118810 for pVS1, AF143682 for pTAR, AF302424 for pVT745, and NC_002142 for pB171. Numbers in parentheses indicate the first nucleotides in these database entries that were included in the primers. Restriction enzyme sites that were used for cloning of amplification products are underlined.

protein (18, 23, 40). These and similar proteins encoded by a range of plasmids form the ParF subgroup of the ParA superfamily. This subgroup is more related evolutionarily to the MinD group of cell division factors than to P1 ParA (18). The partition cassettes of *parF* type plasmids are also distinguished by the absence of *parB*-like genes downstream of *parF*. Instead, these loci encode diverse proteins with sizes of 76 (ParG of TP228), 71 (originally named Orf3, here renamed ParG_{VS1} of pVS1), 94 (ParB_{TAR} of pTAR), 79 (AA15 of pVT745), and 91 (ParB_{B171} of pB171) amino acids (18) (Fig. 1A). Furthermore, these small proteins are apparently unrelated to each other at the primary sequence level, except for the ParG proteins of plasmids TP228 and pVS1, which are sequence and structural homologs (14, 18). These five ParG analogs provide a useful and malleable suite of proteins with which to dissect further the protein-protein and protein-DNA interactions that direct the segregation of *parF* type plasmids.

The ParG, ParB_{TAR}, and ParB_{B171} proteins are necessary for the activity of their cognate partition systems (8, 18, 23). In the case of pTAR, the system is functional in its native host but not in *E. coli* (23); the latter result was replicated here (Table 2). In addition, the *staA-parG_{VS1}* region of plasmid pVS1 promotes the segregational stability of an unstable test vector that replicates by the low-copy-number P1 replicon in *E. coli* (Table 2). In contrast the *parA-aa15* region of plasmid pVT745 did not promote the partition in this background. Considering that the

pVT745 cassette bears the characteristic genetic hallmarks of a partition region (11), it is probable that, like the equivalent pTAR region, the partition locus of pVT745 is active in its native host, although this remains to be verified. Interestingly, the pVT745 replicon is also nonfunctional in *E. coli* (11).

Plasmid partition sites are incompatibility determinants (2). This is most easily explained if plasmids are considered a pool

TABLE 2. Activity of the TP228, pVS1, pTAR, pVT745, and pB171 partition cassettes in *E. coli*

Source of partition region ^a	Plasmid retention in ≈25 generations of nonselective growth (%) ^b
TP228 (<i>parFG</i>)	68 ± 8
pVS1 (<i>staA-parG_{VS1}</i>)	47 ± 18
pTAR (<i>parAB_{TAR}</i>)	<2 ^c
pVT745 (<i>parA-aa15</i>)	<2
pB171 (<i>parAB_{B171}</i>)	46 ± 11
pFH450 (none)	<2

^a Each partition region specifies a ParA homolog (named ParF for TP228 and StaA for pVS1) as well as a ParG analog.

^b The retention levels of P1-based, low-copy-number plasmids containing the indicated partition regions were assessed following growth in the absence of selective pressure for ≈25 generations in the *polA* strain BR825. Averages of at least three individual experiments ± one standard deviation are shown.

^c The pTAR *parAB_{TAR}* system has been demonstrated to be functional in its native host, *A. tumefaciens* (23).

TABLE 3. Incompatibility ratios of the partition cassettes of plasmids TP228, pVS1, pTAR, pVT745, and pB171

Partition cassette present <i>in trans</i> on pUC vector	P1 plasmid retention in ≈ 25 generations of nonselective growth stabilized by partition region ^a :		
	TP228 <i>parFG</i>	pVS1 <i>staA- parG_{VSI}</i>	pB171 <i>parAB</i>
None (pUC18)	1	1	1
TP228 <i>parFG</i>	<0.01	0.07	0.94
pVS1 <i>staA-parG_{VSI}</i>	0.17	0.19	0.70
pTAR <i>parAB_{TAR}</i>	1.13	1.00	1.41
pVT745 <i>parA-aa15</i>	0.98	1.22	1.14
pB171 <i>parAB_{B171}</i>	0.75	0.72	<0.01

^a The retention levels of a P1-based, low-copy-number plasmid stabilized by either the TP228, pVS1, or pB171 partition regions were assessed following growth under nonselective conditions in strain DH5 α for ≈ 25 generations in the presence of coresident pUC-based, high-copy-number plasmids harboring the equivalent regions. Retention is expressed relative to the retention of the P1 plasmid in the presence of pUC18 without a cloned partition cassette. Results are the averages of at least two experiments. Numbers in boldface type highlight values for plasmid pairs with which incompatibility was observed.

from which individuals are withdrawn randomly for pairwise segregation. Plasmids that harbor identical partition sites cannot be distinguished from each other during the partition process, and random assortment ultimately gives rise to populations that have one or the other plasmid but not both (2). Plasmids based on the pUC high-copy-number replication origin and the P1 low-copy-number replicon are compatible and therefore can be used in assessing the incompatibility properties of relevant partition sequences that are cloned in pairs of vectors replicating via these replicons. Plasmids were constructed that replicated via the pUC or P1 origins and which harbored the three partition regions that are active in *E. coli*: *parFG* of TP228, *staA-parG_{VSI}* of pVS1, and *parAB_{B171}* of pB171. Although the partition regions of pTAR and pVT745 are inactive in *E. coli*, these regions were also tested in pUC-based plasmids to assess whether they exerted incompatibility towards the partition-proficient P1-based plasmids. Pairs of plasmids based on the high- and low-copy-number replicons were cotransformed and subsequently grown for ~ 25 generations in the absence of selection for the P1-based plasmid. The partition region of TP228 cloned in pUC expressed self-incompatibility, destabilizing the P1-based plasmid harboring the same region (Table 3) and confirming its incompatibility properties (18). Similarly, the self-incompatibility of the pB171 partition region was verified (8). Interestingly, the partition locus of pVS1 expressed incompatibility both with itself and with the TP228 partition region (Table 3), suggesting that one or more components of the partition systems of these plasmids are interchangeable. In contrast, the pB171 partition cassette was compatible with both the TP228 and pVS1 systems. Neither the pTAR nor pVT745 partition regions exerted incompatibility toward the TP228, pVS1, or pB171 regions.

The ParG analogs of pVS1, pTAR, and pB171 self-associate in vivo. The ParG protein of plasmid TP228 is a homodimer as shown by two-hybrid analysis, chemical cross-linking, analytical ultracentrifugation, and nuclear magnetic resonance studies (4, 14). To investigate the oligomeric state of the equivalent proteins from the additional plasmids under study, a bacterial two-hybrid system based on the reconstitution of a cyclic AMP

signal transduction pathway (24) was employed. In this assay, the proteins under investigation are fused with two fragments, denoted T18 and T25, that form the catalytic domain of the adenylate cyclase of *B. pertussis*. If the test proteins associate, the T18 and T25 polypeptide fragments are brought into sufficiently close proximity to reconstitute adenylate cyclase enzymatic activity and therefore cyclic AMP synthesis in a *cya* strain of *E. coli* (24). Cyclic AMP is a transcriptional activator of a variety of catabolic operons, including the maltose operon. Self-association of the ParG protein can be readily demonstrated in this system (4).

The *parG_{VSI}*, *parB_{TAR}*, *aa15*, and *parB_{B171}* genes were inserted in frame separately with the T18- and T25-encoding fragments. The resulting plasmids were cotransformed into a *cya* mutant of *E. coli*, and transformants were assayed for their phenotypes on MacConkey-maltose agar plates. The colonies containing cognate pairs of T18 and T25 fusion proteins from the pVS1, pTAR, and pB171 plasmids turned red, exhibiting a clear Cya⁺ phenotype after 36 h of growth at 30°C (Fig. 2B, C and E, respectively, sectors 1), whereas control colonies producing either one of the fusion proteins together with the T18 or T25 polypeptide remained white (data not shown). These results indicate that the ParG_{VSI}, ParB_{TAR}, and ParB_{B171} proteins self-associate in vivo. In contrast, the AA15 protein did not detectably self-interact in this system, perhaps because one or both of the fusion proteins is either misfolded or is prevented from oligomerization by the fused adenylate cyclase component or because the self-interaction is too weak to be detected in the two-hybrid setup (Fig. 2D, sector 1).

ParG analogs of pVS1, pTAR, pVT745, and pB171 are homodimers. The ParG_{VSI}, ParB_{TAR}, AA15, and ParB_{B171} proteins were purified as hexahistidine-tagged proteins and were analyzed with the cross-linking reagent DMP to assess their solution oligomeric state (Fig. 3, left). Each protein was rapidly fixed into covalently bound dimers by DMP. The yields of dimerized species increased as a function of time for at least 30 min, after which they tended to attain a plateau. Weak trimeric or higher-order species were occasionally observed at longer incubation times.

The four proteins were also examined by sedimentation velocity analysis at 60,000 rpm (Fig. 3, right). For all proteins, the data unequivocally fitted best to single species with the following molecular masses (in kilodaltons): ParG_{VSI}, 15.8; ParB_{TAR}, 23.4; AA15, 22.0; ParB_{B171}, 23.4. These are in good agreement with the predicted dimeric molecular masses of the His-tagged versions of these proteins of 17.0, 22.0, 19.4, and 21.8 kDa, respectively. In summary, the combined two-hybrid, cross-linking, and analytical ultracentrifugation studies clearly illustrate that the ParG_{VSI}, ParB_{TAR}, AA15, and ParB_{B171} proteins are dimeric. In the case of AA15, this self-association was not detectable in vivo but was shown unambiguously in vitro. Thus, although only ParG_{VSI} is a homolog, each of the proteins under study exhibits the same oligomeric state as dimeric ParG.

ParG analogs of TP228, pVS1, pTAR, pVT745, and pB171 do not heterodimerize. As dimerization of the ParG analogs of TP228, pVS1, pTAR, and pB171 can be readily monitored in a bacterial two-hybrid assay (Fig. 2), it was also possible to assess whether the proteins produced stable heterooligomers in vivo. For this purpose, a pT18 derivative containing an in-frame

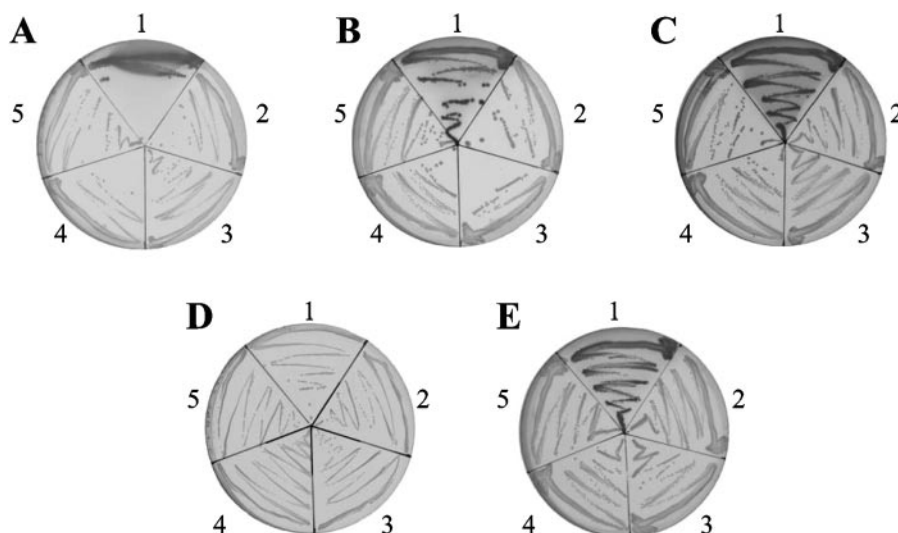


FIG. 2. Bacterial two-hybrid analysis of protein interactions among ParG analogs in the TP228, pVS1, pTAR, pVT745, and pB171 partition systems. Plasmids carrying fusions of *parG* analogs to T25- and T18-encoding fragments were cotransformed into *E. coli* SP850. Transformants were streaked onto MacConkey-maltose plates and incubated at 30°C for 36 h. The strains in the plate sectors contain the following plasmids: A, pT18-ParG plus pT25-ParG (1), pT25-ParB_{B171} (2), pT25-ParB_{TAR} (3), pT25-AA15 (4), or pT25-ParG_{VS1} (5); B, pT18-ParG_{VS1} plus pT25-ParG_{VS1} (1), pT25-ParB_{B171} (2), pT25-ParB_{TAR} (3), pT25-AA15 (4), or pT25-ParG (5); C, pT18-ParB_{TAR} plus pT25-ParB_{TAR} (1), pT25-ParB_{B171} (2), pT25-AA15 (3), pT25-ParG_{VS1} (4), or pT25-ParG (5); D, pT18-AA15 plus pT25-AA15 (1), pT25-ParB_{B171} (2), pT25-ParB_{TAR} (3), pT25-ParG_{VS1} (4), or pT25-ParG (5); E, pT18-ParB_{B171} plus pT25-ParB_{B171} (1), pT25-ParB_{TAR} (2), pT25-AA15 (3), pT25-ParG_{VS1} (4), or pT25-ParG (5).

fusion of the test gene with the T18-encoding fragment of adenylate cyclase was cotransformed separately into strain SP850 with pT25 derivatives containing fusions of either the cognate or noncognate test genes with the T25-encoding fragment. Interaction tests were performed as described previously. The ParG analogs of TP228, pVS1, pTAR, and pB171 were unable to heterodimerize detectably with the noncognate proteins, even during prolonged incubation of the test colonies (Fig. 2A, B, C, and E, respectively). This was the case even for the sequence and structural homologs, ParG and ParG_{VS1} (Fig. 2A and B). The AA15 protein of plasmid pVT745 is a dimer (Fig. 3), but this interaction is not evident in the bacterial two-hybrid assay. Similarly, no interaction between AA15 and the ParG, ParG_{VS1}, ParB_{TAR}, or ParB_{B171} proteins was apparent in this system (Fig. 2D).

Secondary structure analysis of ParG_{VS1}, ParB_{TAR}, AA15, and ParB_{B171}. The secondary structures of the ParG_{VS1}, ParB_{TAR}, AA15, and ParB_{B171} proteins were examined by circular dichroism spectroscopy. The shapes of the profiles in each instance demonstrated minima at 200 to 210 nm, characteristic of proteins with significant α -helical content (Fig. 4A). Secondary structure predictions with CONTIN and CDSSTR software confirmed that the proteins were folded and suggested that the α -helical contents were \sim 20% for ParB_{TAR}, \sim 25% for AA15, \sim 30% for ParG_{VS1}, and \sim 40% for ParB_{B171} (Fig. 4B). Apart from ParB_{B171}, each of the proteins also contained significant quantities of β -strand structure. The dimeric ParG_{VS1} protein is predicted to consist of a C-terminal ribbon-helix-helix domain and a pair of unstructured N-terminal tails. Based on this structure, ParG_{VS1} has been estimated to have an α -helix content comparable to that observed in circular dichroism spectroscopy (14). Similarly, the β -strand

contents of ParG_{VS1} estimated from circular dichroism (Fig. 4B) and from structural alignment with the ParG protein (14) also agree very closely.

For the ParG_{VS1}, ParB_{TAR}, AA15, and ParB_{B171} proteins, it is striking that each is predicted to contain $>$ 40% of unordered residues. Interestingly, \sim 40% of the dimeric ParG protein is located in a pair of flexible N-terminal domains (14). These unstructured tails are crucial for the assembly of higher-order protein-DNA complexes (E. Carmelo et al., submitted for publication). It remains to be elucidated whether the unordered residues in the unrelated ParB_{TAR}, AA15, and ParB_{B171} proteins fulfill a similar function, although more detailed structural analysis is required to verify precisely the amounts of unstructured regions present in these proteins.

ParG analogs of pVS1, pVT745, and pB171 are site-specific DNA-binding proteins. ParG and ParB_{TAR} are DNA-binding proteins that associate with the regions positioned upstream of the associated *parF* homologs (4, 23). These regions harbor characteristic repeat motifs (Fig. 1B) that comprise partition and transcriptional regulatory sites (4, 23; Carmelo et al., submitted). To assess whether the additional proteins under analysis here were also DNA-binding factors, the proteins were tested in gel retardation assays with the equivalent DNA regions from their cognate partition loci. For this purpose, PCR fragments biotinylated at their 5' ends were produced. In each case, these substrates encompassed \sim 250 to 300 bp upstream of the *parF* initiation codons. The ParG_{VS1} protein bound to the region upstream of its *parF* homolog, forming a smear of nucleoprotein complexes that were progressively retarded with increasing protein concentration (Fig. 5). The AA15 and ParB_{B171} proteins exhibited comparable DNA-binding patterns with their cognate sites, although ParB_{B171} produced a

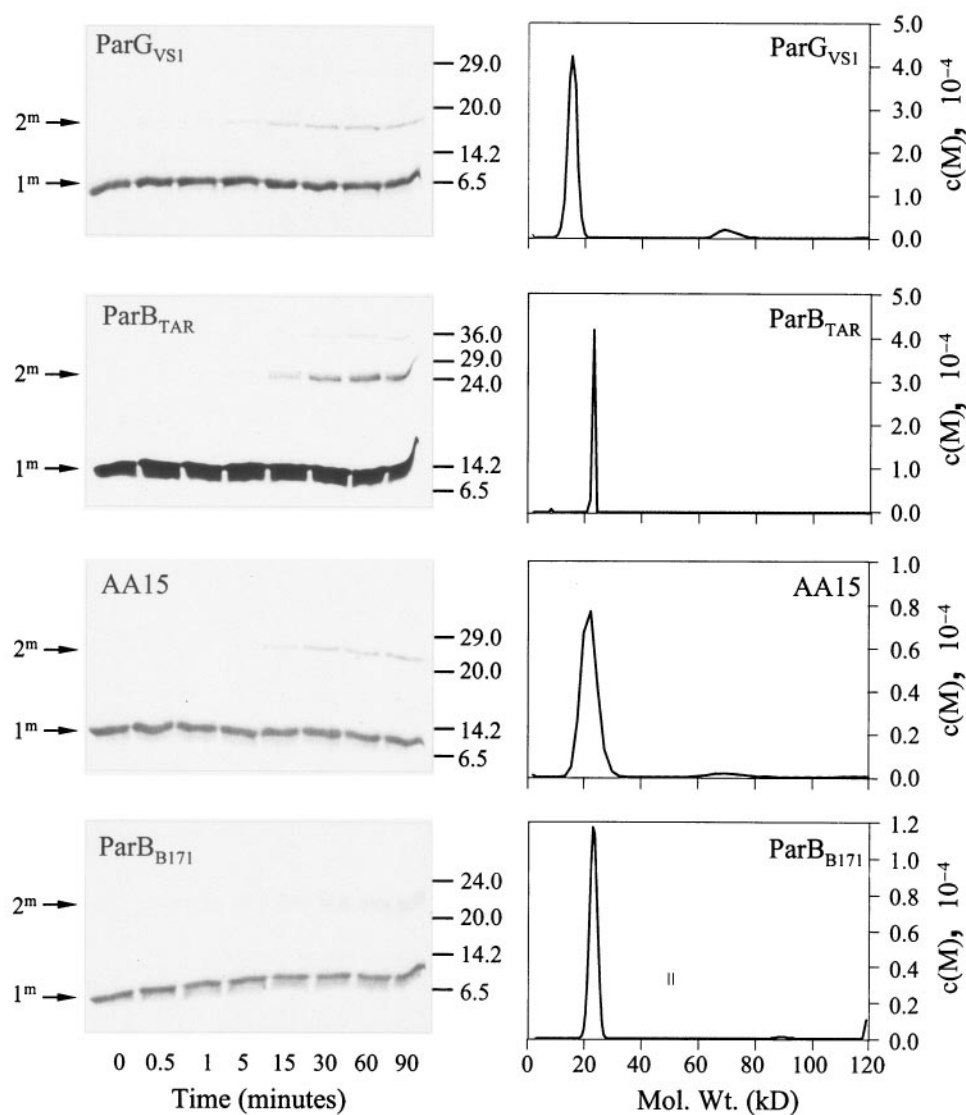
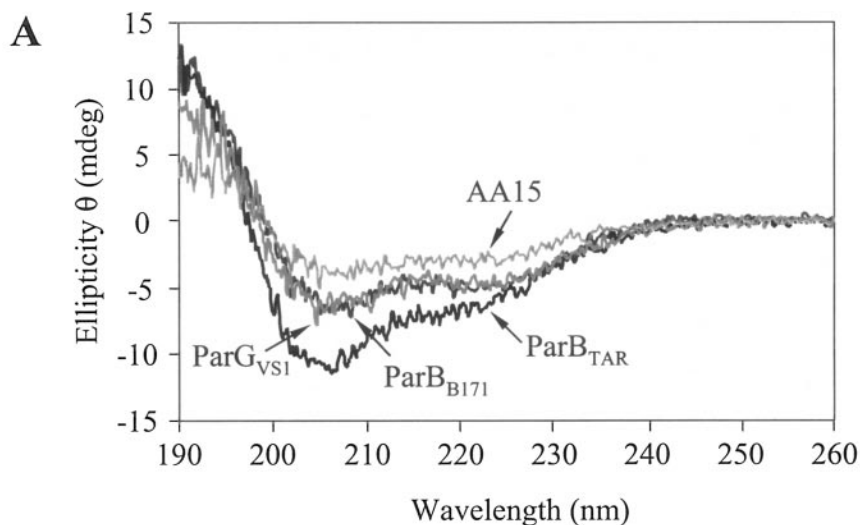


FIG. 3. Analysis of the solution oligomeric state of the ParG_{VS1}, ParB_{TAR}, AA15, and ParB_{B171} proteins. The left panels show time course reactions of cross-linking with DMP for each protein. The positions of monomeric (1^m) and dimeric (2^m) species are indicated on the left; molecular mass markers (kDa) are shown on the right. The right panels show sedimentation velocity profiles of the four proteins. Proteins were subjected to ultracentrifugation at a speed of 60,000 rpm (Optima XL-1 ultracentrifuge; Beckman) and a temperature of 23°C. The data were analyzed as described in Materials and Methods. In each case, a predominant species at the dimeric position is evident.

discrete complex at the lowest protein concentrations that were used. The interactions of the ParG_{VS1}, AA15, and ParB_{B171} proteins with their cognate sites are specific, as, like ParG, they did not bind to an unrelated segment of DNA at protein concentrations that were sufficient to shift the cognate substrate completely (data not shown). The patterns of diffuse protein-DNA complexes observed with ParG_{VS1}, AA15, and ParB_{B171} are very similar to those previously observed with ParG and ParB_{TAR}; the latter are reproduced here for comparison (Fig. 5). The substrate fragments include multiple-repeat sequences that are the probable recognition motifs for the cognate proteins (Fig. 1). The distinctive smeared nucleoprotein complexes noted for all five proteins may reflect the progressive occupation by the proteins of different numbers of

these motifs. However, the minimal protein concentrations that are required to fully bind the substrates differ between the proteins, suggesting that the affinities of the proteins for their cognate sites may be dissimilar. In summary, the results show that ParG_{VS1}, AA15, and ParB_{B171} are DNA-binding proteins that recognize specific sequences in the regions upstream of the cognate *parF* genes.

Specificity of the protein-DNA interactions mediated by ParG, ParG_{VS1}, ParB_{TAR}, AA15, and ParB_{B171}. The ParG, ParG_{VS1}, ParB_{TAR}, AA15, and ParB_{B171} proteins are nonexchangeable homodimeric proteins that bind to the regions located upstream of the associated *parF* genes. To determine whether these proteins also recognize the noncognate partition loci or are specific for their associated sites, gel retardation



Protein	Secondary structure prediction (%) ^a					
	α_R	α_D	β_R	β_D	T	U
ParG _{VS1}	17	12	9	6	14	42
ParB _{TAR}	10	8	13	8	16	45
AA15	12	11	12	7	16	41
ParB _{B171}	25	15	0	4	13	43

^a α_R , α -helix; α_D , distorted α -helix; β_R , β -strand; β_D , distorted β -strand; T, turns; U, unordered

FIG. 4. Circular dichroism spectroscopy of the ParG_{VS1}, ParB_{TAR}, AA15, and ParB_{B171} proteins. (A) Superimposed far-UV spectra of the four proteins. (B) The deconvoluted data in panel A were used to make estimations of the secondary structure content of each protein with the CONTIN prediction program. Analysis with the CDSSTR program yielded comparable results (data not shown).

assays were conducted in which each binding site was tested with each partition protein in turn. The ParG protein binds to DNA nonspecifically at elevated protein concentrations (14), and the same observation was made with some of the additional proteins tested here (data not shown). To circumvent this potential problem, the proteins were used at concentrations that are just sufficient to convert the free substrate into fully bound complex by the cognate DNA-binding protein. This analysis revealed that the related ParG and ParG_{VS1} proteins efficiently bound both the cognate and alternative substrates (Fig. 6A and B). However, the electrophoretic migrations of nucleoprotein complexes containing the same substrate were quite different between the two proteins. ParG_{VS1} also bound the substrate derived from the pVT745 partition region (Fig. 6D). Thus, the ParG_{VS1} protein interacted with

three of the five substrate DNAs, although there are no obvious similarities between the repeat sequences within these three substrates that are the candidate recognition sites for their cognate proteins (Fig. 1). Further analysis with enzymatic or chemical footprinting techniques is required to probe the ParG_{VS1} interactions in more detail.

Another instance of interchangeability was evident with the substrate derived from plasmid pB171 with which both ParB_{B171} and AA15 interacted (Fig. 6E). In contrast, ParB_{B171} did not bind the fragment derived from pVT745 (Fig. 6D). The ParB_{TAR} protein was entirely specific for its cognate substrate, and no other partition protein interacted with this site (Fig. 6C).

In summary, mixing and matching of the suite of partition proteins and their DNA sites revealed that the related ParG

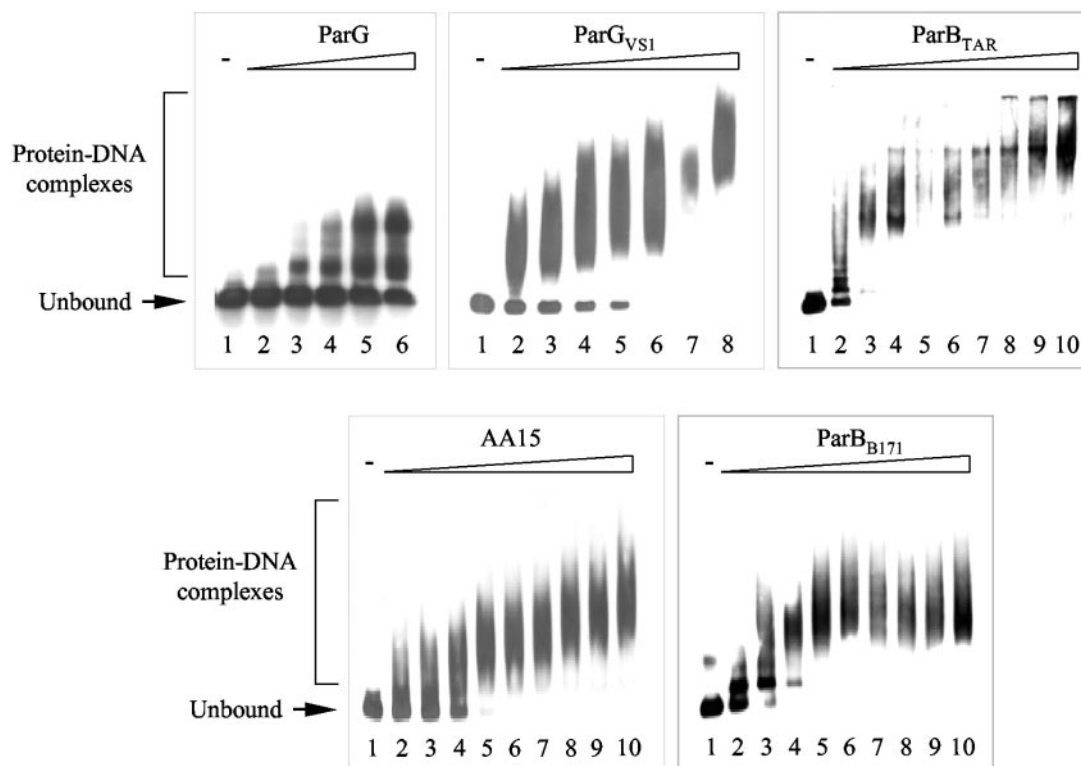


FIG. 5. Protein-DNA interactions of the ParG_{VS1}, ParB_{TAR}, AA15, and ParB_{B171} proteins. The indicated proteins were used in binding reactions with the biotinylated DNA sequences (2 nM) located upstream of their cognate *parF* genes and analyzed as described in Materials and Methods. These sequences include the repeat motifs shown in Fig. 1. The micromolar protein concentrations used were as follows. ParG lanes: 1, 0.0; 2, 0.05; 3, 0.10; 4, 0.15; 5, 0.26; 6, 0.52. ParG_{VS1} lanes: 1, 0.0; 2, 2.5; 3, 5.0; 4, 6.0; 5, 7.0; 6, 8.0; 7, 9.0; 8, 10.0. ParB_{TAR} lanes: 1, 0.0; 2, 0.2; 3, 0.3; 4, 0.4; 5, 0.5; 6, 0.6; 7, 0.7; 8, 0.8; 9, 0.9; 10, 1.0. AA15 lanes: 1, 0.0; 2, 2.0; 3, 3.0; 4, 4.0; 5, 5.0; 6, 6.0; 7, 7.0; 8, 8.0; 9, 9.0; 10, 10.0. ParB_{B171} lanes: 1, 0.0; 2, 0.4; 3, 0.6; 4, 0.8; 5, 1.0; 6, 1.2; 7, 1.4; 8, 1.6; 9, 1.8; 10, 2.0. The interaction of ParG and ParB_{TAR} with their cognate target sites has been demonstrated previously (4, 23), although the ratio of ParB_{TAR} to DNA at which nucleoprotein complex formation was observed is slightly different from that previously described (23).

and ParG_{VS1} proteins can cross-react with the noncognate partition sites, although the conformations of the resulting nucleoprotein complexes may differ between cognate and noncognate proteins bound to the same site. There are also some other instances of cross-reactivity between certain partition proteins and noncognate substrates, but in general, interactions are confined to protein-DNA pairs derived from the same plasmid: 16 of the 20 tested combinations of noncognate protein-DNA pairs were nonproductive (Fig. 6).

DISCUSSION

The prototypical partition regions of plasmids P1 and P7 are colinear and homologous. Both cassettes consist of highly similar *parAB* operons followed by the *cis*-acting partition site, *parS*. Despite the evolutionary proximity of these partition regions, the individual elements of the cassettes are not functionally interchangeable. This specificity is conferred by relatively subtle variations among the P1 and P7 components that are crucial for protein-protein and protein-DNA interactions during segregation (19, 20, 34, 35). The homologous partition regions of plasmids F and N15 similarly exhibit species specificity (36). In contrast, the segregation regions of plasmids TP228, pVS1, pTAR, pVT745, and pB171 display more fundamental differences. In particular, although these plasmids

harbor homologous *parF* genes, the flanking genes that encode DNA-binding factors apparently are unrelated to each other or to *parB*, except for the *parG* genes of TP228 and pVS1, which specify sequence and structural homologs (Fig. 1A). In turn, the sites with which the ParG analogs interact are also apparently different, although similarly located upstream of the homologous *parF* genes.

The TP228 and pVS1 regions are sufficiently similar to exert cross-incompatibility but are fully compatible with the partition systems of pTAR, pVT745, and pB171. The production of ParG heterodimers is an unlikely explanation for the observed incompatibility, as no interaction was evident between ParG and ParG_{VS1} in two-hybrid analysis. More feasibly, the cross-incompatibility shown by the TP228 and pVS1 systems could be explained by the binding of the ParG proteins to the noncognate partition sites (Fig. 6A and B) with subsequent interference with correct partitioning. Interestingly, the relative migrations of the nucleoprotein complexes of ParG and ParG_{VS1} bound to either site are quite different, suggesting that the conformations of these complexes or the protein-DNA stoichiometries within the complexes are dissimilar. The cross-incompatibility expressed by the TP228 and pVS1 partition regions may also be explained by other inappropriate interactions, e.g., by regulation of the partition operons. In contrast,

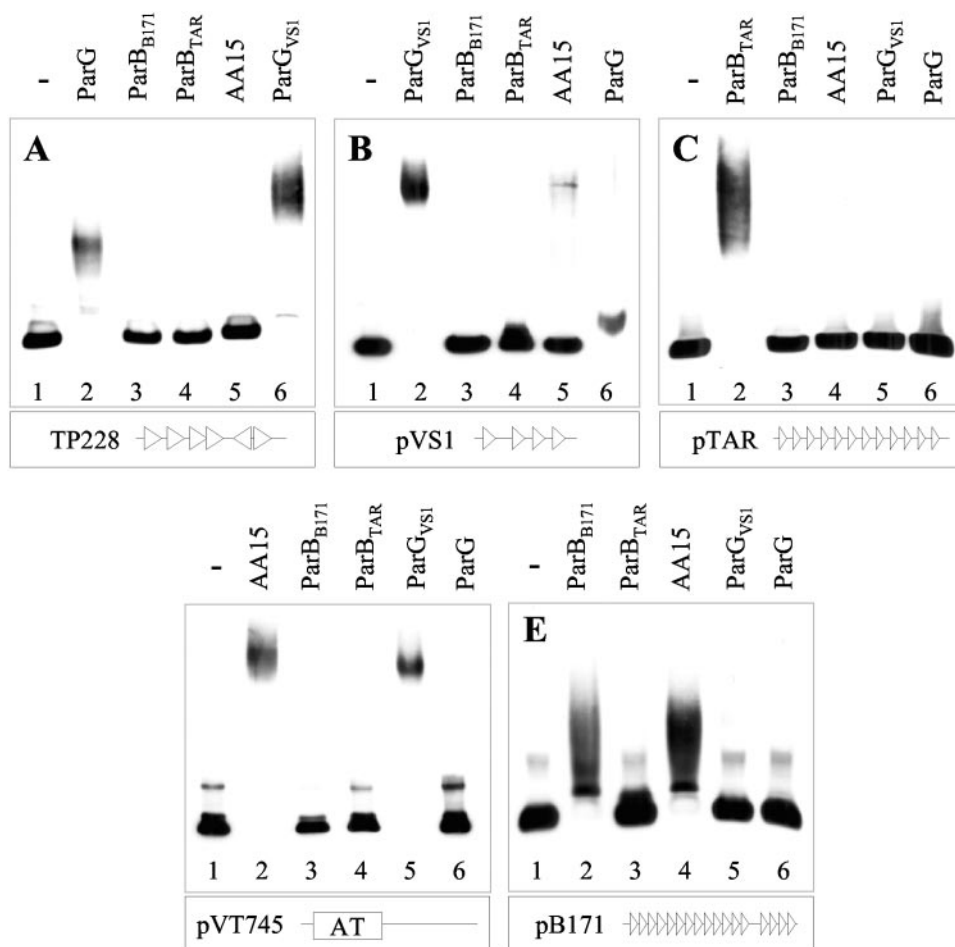


FIG. 6. DNA interaction specificity of the ParG, ParG_{VS1}, ParB_{TAR}, AA15, and ParB_{B171} proteins. The indicated proteins were used in binding reactions with the biotinylated DNA sequences (2 nM) located upstream of the cognate *parF* genes and analyzed as described in Materials and Methods. The substrate DNAs illustrated beneath each panel were derived from TP228 (A), pVS1 (B), pTAR (C), pVT745 (D), and pB171 (E). In each panel, the proteins were used at the following concentrations, which are sufficient to convert the free substrate into fully bound complex by the cognate DNA-binding protein: A, 0.5 μ M; B, 20 μ M; C, 1.0 μ M; D, 20 μ M; E, 1.0 μ M. —, no protein.

ParG_{VS1} bound the putative pVT745 partition site (Fig. 6D), but no partition-mediated incompatibility was apparent between these systems *in vivo* (Table 3).

Although there are notable examples of cross-reactivity between certain ParG analogs and noncognate DNA sites, the protein-DNA interactions among the tested partition systems are remarkably specific overall (Fig. 6). For example, the ParB_{TAR} protein recognizes only its own site, which itself is not bound by any other tested protein. Similarly, ParB_{B171} interacts with its cognate site but not with any other fragment, and ParG is specific for its site apart from cross-reactivity with the pVS1 region. The sequence dissimilarities among the tested ParG analogs and the repeat motifs in their binding sites undoubtedly have evolved as a strategy to ensure that coresident plasmids harboring these diverse partition regions are maintained and distributed accurately. Thus, the ParG analogs bind specifically to their cognate partition sites upstream of the corresponding *parF* genes and function as specificity determinants by facilitating the partition of the replicon from which they are derived but not necessarily of other replicons that may harbor a *parF* gene. The common ParF proteins in each case

may act as a scaffold which attaches the nucleoprotein complex to a host partition apparatus, although specific interactions between ParF and the ParG analogs may also be involved (T. J. G. Fothergill and F. Hayes, unpublished data). Therefore, although the nucleoprotein complexes formed at the partition sites may consist of analogous elements, the individual components may be plasmid specific and noninterchangeable. The targeting of different plasmids to distinctive subcellular locations may also play a role in ensuring the efficient segregation of compatible plasmids (22). It should also be noted that the observed DNA binding by the partition proteins could represent a combination of partition site binding and interaction with autoregulatory sites.

The tested ParG analogs are all dimeric and contain significant quantities of α -helix structure and unordered residues. The ParB_{B171} protein seems most dissimilar, as it has the highest α -helix and lowest β -strand contents. The DNA-binding proteins in plasmid partition systems generally are dimeric (3, 4, 10, 16), which likely reflects their interaction with palindromic DNA sites that can be embedded within direct repeat motifs such as those illustrated in Fig. 1. Among the ParG

analogs, only the modes of binding by ParG and, by inference, ParG_{VS1} are understood. The C-terminal domains within the ParG dimer interleave into a ribbon-helix-helix fold in which the double-stranded β -sheets are predicted to insert in the major groove of DNA (14). The ParB_{TAR}, AA15, and ParB_{B171} proteins are not obviously ribbon-helix-helix proteins, so they presumably interact with DNA by a different mechanism. In addition to its interfolded C-terminal domains, dimeric ParG contains a pair of unstructured N-terminal tails (~30 residues each) which are crucial for the formation of higher-order nucleoprotein complexes (Carmelo et al., submitted). Intriguingly, the ParG analogs are similarly predicted to harbor significant quantities of unordered residues, although it remains to be assessed whether these residues are contiguous and perform a similar function.

Apart from ParG_{VS1}, ParG possesses a variety of plasmid-specified homologs (14, 18, 25). Similarly, the *Zymomonas* chromosome and certain *Pseudomonas* and *Xanthomonas* plasmids encode ParB_{TAR} and ParB_{B171} homologs, respectively (data not shown). Furthermore, the proteins examined in this study are not an exhaustive set of ParG analogs: other, distinct analogs have also been identified (18). Thus, the systems described here that consist of ParF homologs accompanied by diverse ParG analogs which bind to their cognate partition sites are widely used among plasmids of gram-negative bacteria as active partition systems; their continued analysis will provide new vistas on the events involved in stable plasmid segregation.

ACKNOWLEDGMENTS

This work was funded by grants from The Wellcome Trust and Biotechnology and Biological Sciences Research Council to F.H. T.J.G.F. was supported by a UMIST Life Sciences Initiative Studentship. D.B. is a Medical Research Council New Investigator.

We thank Dominique Galli, Stephan Heeb, Toru Tobe, and Michael Yarmolinsky for generous gifts of plasmids without which the work described here would not have been possible; Andy Baron for expert assistance with analytical ultracentrifugation studies; and Andrew Doig for providing access to the spectropolarimeter.

REFERENCES

- Alberts, B. 1998. The cell as a collection of protein machines: preparing the next generation of molecular biologists. *Cell* **92**:291–294.
- Austin, S., and K. Nordstrom. 1990. Partition-mediated incompatibility of bacterial plasmids. *Cell* **60**:351–354.
- Balzer, D., G. Ziegelin, W. Pansegrau, V. Kruff, and E. Lanka. 1992. KorB protein of promiscuous plasmid RP4 recognizes inverted sequence repetitions in regions essential for conjugative plasmid transfer. *Nucleic Acids Res.* **20**:1851–1858.
- Barillà, D., and F. Hayes. 2003. Architecture of the ParF-ParG protein complex involved in prokaryotic DNA segregation. *Mol. Microbiol.* **49**:487–499.
- Benos, P. V., A. S. Lapedes, and G. D. Stormo. 2002. Is there a code for protein-DNA recognition? *Probab(ilistical)ly*. . . *Bioessays* **24**:466–475.
- Bouet, J. Y., and B. E. Funnell. 1999. P1 ParA interacts with the P1 partition complex at parS and an ATP-ADP switch controls ParA activities. *EMBO J.* **18**:1415–1424.
- Compton, L. A., and W. C. Johnson, Jr. 1986. Analysis of protein circular dichroism spectra for secondary structure using a simple matrix multiplication. *Anal. Biochem.* **155**:155–167.
- Ebersbach, G., and K. Gerdes. 2001. The double *par* locus of virulence factor pB171: DNA segregation is correlated with oscillation of ParA. *Proc. Natl. Acad. Sci. USA* **98**:15078–15083.
- Erdmann, N., T. Petroff, and B. E. Funnell. 1999. Intracellular localization of P1 ParB protein depends on ParA and *parS*. *Proc. Natl. Acad. Sci. USA* **96**:14905–14910.
- Funnell, B. E. 1991. The P1 plasmid partition complex at *parS*. The influence of *Escherichia coli* integration host factor and of substrate topology. *J. Biol. Chem.* **266**:14328–14337.
- Galli, D. M., J. Chen, K. F. Novak, and D. J. LeBlanc. 2001. Nucleotide sequence and analysis of conjugative plasmid pVT745. *J. Bacteriol.* **183**:1585–1594.
- Gallie, D. R., and C. I. Kado. 1987. *Agrobacterium tumefaciens* pTAR *parA* promoter region involved in autoregulation, incompatibility and plasmid partitioning. *J. Mol. Biol.* **193**:465–478.
- Gallie, D. R., S. Novak, and C. I. Kado. 1985. Novel high- and low-copy stable cosmids for use in *Agrobacterium* and *Rhizobium*. *Plasmid* **14**:171–175.
- Golovanov, A. P., D. Barillà, M. Golovanova, F. Hayes, and L.-Y. Lian. 2003. ParG, a protein required for active partition of bacterial plasmids, has a dimeric ribbon-helix-helix structure. *Mol. Microbiol.* **50**:1141–1153.
- Gordon, G. S., D. Sitnikov, C. D. Webb, A. Teleman, A. Straight, R. Losick, A. W. Murray, and A. Wright. 1997. Chromosome and low copy plasmid segregation in *E. coli*: visual evidence for distinct mechanisms. *Cell* **90**:1113–1121.
- Hanai, R., R. Liu, P. Benedetti, P. R. Caron, A. S. Lynch, and J. C. Wang. 1996. Molecular dissection of a protein SopB essential for *Escherichia coli* F plasmid partition. *J. Biol. Chem.* **271**:17469–17475.
- Hayes, F. 1980. A family of stability determinants in pathogenic bacteria. *J. Bacteriol.* **180**:6415–6418.
- Hayes, F. 2000. The partition system of multidrug resistance plasmid TP228 includes a novel protein that epitomizes an evolutionarily distinct subgroup of the ParA superfamily. *Mol. Microbiol.* **37**:528–541.
- Hayes, F., and S. J. Austin. 1993. Specificity determinants of the P1 and P7 plasmid centromere analogs. *Proc. Natl. Acad. Sci. USA* **90**:9228–9232.
- Hayes, F., L. Radnedge, M. A. Davis, and S. J. Austin. 1994. The homologous operators for P1 and P7 plasmid partition are autoregulated from dissimilar operator sites. *Mol. Microbiol.* **11**:249–260.
- Heeb, S., Y. Itoh, T. Nishijyo, U. Schneider, C. Keel, J. Wade, U. Walsh, F. O'Gara, and D. Haas. 2000. Small, stable shuttle vectors based on the minimal pVS1 replicon for use in gram-negative, plant-associated bacteria. *Mol. Plant Microbe Interact.* **13**:232–237.
- Ho, T. Q., Z. Zhong, S. Aung, and J. Pogliano. 2002. Compatible bacterial plasmids are targeted to independent cellular locations in *Escherichia coli*. *EMBO J.* **21**:1864–1872.
- Kalnin, K., S. Stegalkina, and M. Yarmolinsky. 2000. pTAR-encoded proteins in plasmid partitioning. *J. Bacteriol.* **182**:1889–1894.
- Karimova, G., J. Pidoux, A. Ullmann, and D. Ladant. 1998. A bacterial two-hybrid system based on a reconstituted signal transduction pathway. *Proc. Natl. Acad. Sci. USA* **95**:5752–5756.
- Kwong, S. M., C. C. Ye, and C. L. Poh. 2001. Molecular analysis of the pRA2 partitioning region: ParB autoregulates *parAB* transcription and forms a nucleoprotein complex with the plasmid partition site, *parS*. *Mol. Microbiol.* **40**:621–633.
- Li, Y., and S. Austin. 2002. The P1 plasmid is segregated to daughter cells by a 'capture and ejection' mechanism coordinated with *Escherichia coli* cell division. *Mol. Microbiol.* **46**:63–74.
- Li, Y., A. Dabrazhynetskaya, B. Youngren, and S. Austin. 2004. The role of Par proteins in the active segregation of the P1 plasmid. *Mol. Microbiol.* **53**:93–102.
- Lobley, A., L. Whitmore, and B. A. Wallace. 2002. DICHROWEB: an interactive website for the analysis of protein secondary structure from circular dichroism spectra. *Bioinformatics* **18**:211–212.
- Ludtke, D. N., B. G. Eichorn, and S. J. Austin. 1989. Plasmid-partition functions of the P7 prophage. *J. Mol. Biol.* **209**:393–406.
- Nooren, I. M., and J. M. Thornton. 2003. Diversity of protein-protein interactions. *EMBO J.* **22**:3486–3492.
- Novak, K. F., and D. J. LeBlanc. 1994. Characterization of plasmid pVT745 isolated from *Actinobacillus actinomycetemcomitans*. *Plasmid* **31**:31–39.
- Philo, J. S. 2000. A method for directly fitting the time derivative of sedimentation velocity data and an alternative algorithm for calculating sedimentation coefficient distribution functions. *Anal. Biochem.* **279**:151–163.
- Provencher, S. W., and J. Glockner. 1981. Estimation of protein secondary structure from circular dichroism. *Biochemistry* **20**:33–37.
- Radnedge, L., M. A. Davis, and S. J. Austin. 1996. P1 and P7 plasmid partition: ParB protein bound to its partition site makes a separate discriminator contact with the DNA that determines species specificity. *EMBO J.* **15**:1155–1162.
- Radnedge, L., B. Youngren, M. Davis, and S. Austin. 1998. Probing the structure of complex macromolecular interactions by homolog specificity scanning: the P1 and P7 plasmid partition systems. *EMBO J.* **17**:6076–6085.
- Ravin, N. V., J. Rech, and D. Lane. 2003. Mapping of functional domains in F plasmid partition proteins reveals a bipartite SopB-recognition domain in SopA. *J. Mol. Biol.* **329**:875–889.
- Shah, S., and A. Peterkofsky. 1991. Characterization and generation of *Escherichia coli* adenylate cyclase deletion mutants. *J. Bacteriol.* **173**:3238–3242.
- Sreerama, N., and R. W. Woody. 2000. Estimation of protein secondary structure from CD spectra: comparison of CONTIN, SELCON and CDSSTR methods with an expanded reference set. *Anal. Biochem.* **287**:252–260.

39. **Surtees, J. A., and B. E. Funnell.** 2003. Plasmid and chromosome traffic control: how ParA and ParB drive partition. *Curr. Top. Dev. Biol.* **56**:145–180.
40. **Tobe, T., T. Hayashi, C. G. Han, G. K. Schoolnik, E. Ohtsubo, and C. Sasakawa.** 1999. Complete DNA sequence and structural analysis of the enteropathogenic *Escherichia coli* adherence factor plasmid. *Infect. Immun.* **67**:5455–5462.
41. **Whitmore, L., and B. A. Wallace.** 2004. DICHROWEB, an online server for protein secondary structure analyses from circular dichroism spectroscopic data. *Nucleic Acids Res.* **32**:W668–673.
42. **Woodcock, D. M., P. J. Crowther, J. Doherty, S. Jefferson, E. Decruz, M. Noyer-Weidner, S. S. Smith, M. Z. Michael, and M. W. Graham.** 1989. Quantitative evaluation of *Escherichia coli* host strains for tolerance to cytosine methylation in plasmid and phage recombinants. *Nucleic Acids Res.* **17**:3469–3478.
43. **Yang, W., and G. D. van Duyn.** 2004. Protein-nucleic acid interactions. *Curr. Opin. Struct. Biol.* **14**:1–3.
44. **Yanisch-Perron, C., J. Vieira, and J. Messing.** 1985. Improved M13 phage cloning vectors and host strains: nucleotide sequences of the M13mp18 and pUC19 vectors. *Gene* **33**:103–119.